

Differentiation of Hodgkin lymphoma cells by reactive oxygen species and regulation by heme oxygenase-1 through HIF-1 α

Makoto Nakashima¹ | Mariko Watanabe² | Kazumi Nakano¹ | Kaoru Uchimarū¹ | Ryouichi Horie² 

¹Laboratory of Tumor Cell Biology, Department of Computational Biology and Medical Sciences, Graduate School of Frontier Sciences, The University of Tokyo, Tokyo, Japan

²Division of Hematology, Department of Laboratory Sciences, School of Allied Health Sciences, Kitasato University, Sagami-hara, Japan

Correspondence

Ryouichi Horie, Division of Hematology, Department of Laboratory Sciences, School of Allied Health Sciences, Kitasato University, 1-15-1 Kitasato, Minami-ku, Sagami-hara, Kanagawa 252-0373, Japan. Email: rhorie@med.kitasato-u.ac.jp

Funding information

Japan Agency for Medical Research and Development, Grant/Award Number: 19fk0108039h0003 and 20fk0108126h0001; Japan Society for the Promotion of Science, Grant/Award Number: 17K08728, 19K07442, 19K16580 and 20K07379

Abstract

We previously indicated that Hodgkin lymphoma (HL) cells contain a small side population (SP) that differentiate into a large major population (MP) with giant Hodgkin and Reed-Sternberg (H and RS)-like cells. However, its molecular mechanisms are not fully understood. In this study, we found that intracellular reactive oxygen species (ROS) are low in the SP compared to the MP. Hydrogen peroxide induces large H- and RS-like cells in HL cell lines, but induces cell death in unrelated lymphoid cell lines. Microarray analyses revealed the enrichment of upregulated genes under hypoxic conditions in the SP compared to the MP, and we verified that the SP cells are hypoxic. Hypoxia inducible factor (HIF)-1 α was preferentially expressed in the SP. CoCl₂, a HIF-1 α stabilizer, blunted the effect of hydrogen peroxide. Heme oxygenase-1 (HO-1), a scavenger of ROS, was triggered by HIF-1 α . The effect of hydrogen peroxide was inhibited by HO-1 induction, whereas it was promoted by HO-1 knockdown. HO-1 inhibition by zinc protoporphyrin promoted the differentiation and increased ROS. These results stress the unique roles of ROS in the differentiation of HL cells. Immature HL cells are inhibited from differentiation by a reduction of ROS through the induction of HO-1 via HIF-1 α . The breakdown of this might cause the accumulation of intracellular ROS, resulting in the promotion of HL cell differentiation.

KEYWORDS

differentiation, heme oxygenase-1, Hodgkin lymphoma, hypoxia inducible factor 1, oxygen species

1 | INTRODUCTION

Although Hodgkin and Reed-Sternberg (H and RS) cells characterize Hodgkin lymphoma (HL), we and other groups have found that HL cells consist of heterogeneous subpopulations that include precursor cells with stem cell-like phenotypes.^{1,2} We previously reported that in addition to H and RS cells, HL contains mononuclear small and large cells. HL cell lines contain a side population (SP) that

represents a stem cell-like phenotype, and this fraction consists of mononuclear small cells. The SP cells differentiate into relatively large major population (MP) cells containing H- and RS-like cells.² Another report also showed that mononuclear cells generate multinuclear cells and that a portion of mononuclear cells possesses several phenotypes of cancer-initiating cells.^{1,3} However, the molecular mechanisms underlying the differentiation of HL cells are still not fully understood.

This is an open access article under the terms of the Creative Commons Attribution-NonCommercial License, which permits use, distribution and reproduction in any medium, provided the original work is properly cited and is not used for commercial purposes.

© 2021 The Authors. *Cancer Science* published by John Wiley & Sons Australia, Ltd on behalf of Japanese Cancer Association.

Reactive oxygen species (ROS) are a general name for the highly reactive byproducts of aerobic metabolism, including hydrogen peroxide, hypochlorite ions, superoxide anions, and hydroxyl radicals. ROS damage cellular components such as lipids, proteins, and DNA, which cause cellular dysfunction. However, cellular defense systems protect against the harmful action of ROS by metabolizing them into less harmful molecules.⁴

Mitochondria are a major source of ROS. Mitochondria produce ATP efficiently by aerobic respiration using pyruvate and NADH generated by glycolysis. However, the generation of ROS occurs during this process as a byproduct. Such ROS can damage mitochondria, causing their dysfunction and accelerating ROS production.⁵

The tight regulation of ROS is important to maintain the properties of stem cells, and its deregulation triggers pleiotropic effects such as proliferation, differentiation, senescence, and apoptosis.^{6,7} The increased production of ROS and altered redox status are observed in cancer cells.⁸ A previous report showed that the concentration of intracellular ROS is variable in HL cell lines, and their concentration is low in small mononuclear cells with cancer-initiating cell-like phenotypes.³ A recent report also showed that hydrogen peroxide induces a senescent phenotype in HL cell lines.⁹

In this study, to address how HL cells differentiate, we examined the roles of ROS and its regulation. We found that ROS is closely involved in the differentiation of HL cells and is regulated by heme oxygenase-1 (HO-1) through hypoxia inducible factor (HIF)-1 α .

2 | MATERIALS AND METHODS

2.1 | Cell lines and cell cultures

HL cell lines (L428, KMH2, HDLM2, and L540) were purchased from the German Collection of Microorganisms and Cell Cultures. B-cell lines (Namalwa, BJAB, and Ramos) and a T-cell line (Jurkat) were purchased from the Japanese Cancer Research Resources Bank and RIKEN BioResource Research Center, respectively. Cells were cultured in RPMI 1640 supplemented with 10% or 20% fetal bovine serum (FBS) and antibiotics.

2.2 | Chemicals

Hydrogen peroxide, one of ROS, was purchased from Wako and used for experiments at the specified concentrations.¹⁰ Zinc protoporphyrin (znpp), an inhibitor of HO-1, was purchased from EMD Millipore and used at the specified concentrations.¹¹ Echinomycin, an inhibitor of HIF-1 α ,¹² was purchased from Sigma-Aldrich. CoCl₂, which stabilizes HIF-1 α by inhibiting its degradation, was purchased from Iwai Chemicals Company Ltd. Jietacin A, an NF- κ B inhibitor, which inhibits nuclear translocation of NF- κ B¹³ was kindly provided by Dr T. Sunazuka at Kitasato University.

2.3 | Immunostaining

Fluorescence immunostaining of cell lines was performed as previously described.¹⁴ Antibodies used were anti-HIF-1 α antibody, ab16066 (Abcam); anti-mitochondria antibody, ab92824 (Abcam); anti-heme oxygenase-1 antibody, D-8 (Santa Cruz Biotechnology); anti-FoxO3a, #12829 (Cell Signaling Technology); anti-active NF- κ B, which recognizes the uncovered nuclear localization signal of RelA (Chemicon International); and anti-mouse IgG secondary antibody conjugated with Alexa Fluor 488 (Life Technologies).

Double staining of CD30 and HIF-1 α was performed on paraffin-embedded specimens of cell lines or primary clinical samples with the approval of the ethics committee of Kitasato University. After deparaffinization, samples were subjected to autoclave antigen retrieval in 10 mmol/L citrate buffer (pH 6.0). The sections were blocked using 1% bovine serum albumin (BSA) for 20 min and incubated with anti-HIF-1 α antibody, GTX127309 (Gene Tex Inc.), and anti-CD30 antibody, clone Ber-H2 (Agilent Technologies Inc.) at 4°C overnight. Sections were then washed and further incubated with goat-anti-mouse IgG (H + L) Alexa Fluor 555 and goat-anti-rabbit IgG (H + L) Alexa Fluor 488 for 1 h. After washing with PBS, the sections were treated with Autofluorescence Quenching kit (Vector TrueVIEW, VECTOR Laboratories Inc.). Signals were detected using a fluorescence microscope (HS All-in-one Fluorescence Microscope-BZ-9000; KEYENCE).

2.4 | Measurement of ploidy

Hoechst 33342 (4 μ g/mL; Sigma-Aldrich) and verapamil (7.5 μ g/mL; Sigma-Aldrich) were added in the cell culture medium with cells (5.0×10^5) for 1 h at 37°C, then they were counterstained with 0.5 μ g/mL propidium iodide (PI, Sigma-Aldrich) to label dead cells. The ploidy was analyzed by FACS Aria or Verse (BD Biosciences) equipped with a UV laser or violet laser (350 nm or 407 nm excitation) and FlowJo (BD Biosciences).

2.5 | SP analysis

SP analysis was performed as previously described.² Briefly, cells (1.0×10^6) were incubated with 4 μ g/mL (for KMH2) or 7 μ g/mL (for L428) of Hoechst 33342 dye at 37°C for 1 h, with or without 30 μ g/mL verapamil (Sigma-Aldrich). The cells were counterstained with 0.5 μ g/mL PI and analyzed with FACS Aria as described.²

2.6 | Detection of intracellular ROS and mitochondrial ROS production

To detect intracellular ROS or mitochondrial ROS production, cells (2.5×10^5) were cultured with 10 μ mol/L of CM-H₂DCFDA (5-(*and*-6)-chloromethyl-2,7-dichlorofluorescein diacetate acetyl ester) or

2 $\mu\text{mol/L}$ of MitoTracker Red CM-H₂XRos (both from Thermo Fisher Scientific), respectively, for 40 min at 37°C. CM-H₂DCFDA distributes intracellularly, fluoresces upon oxidation, and is used to detect intracellular ROS. MitoTracker Red CM-H₂XRos is a probe specific for mitochondria that fluoresces on oxidation and is used to detect mitochondrial ROS. Hoechst 33342 staining for SP detection was performed for 60 min at 37°C. The cells were analyzed by FACS Aria or FACS Verse, and FlowJo (both BD Biosciences).

2.7 | Detection of hypoxic cells

To examine the oxygen status of SP cells, cells (5.0×10^5) were cultured with 1 $\mu\text{mol/L}$ of Hypoxia Green Reagent for Flow Cytometry (Thermo Fisher Scientific) at 37°C in a Multigas incubator (MCO-18M, SANYO Electric Biomedical Co., Ltd). At the point of 2 h, 3 $\mu\text{g/mL}$ of Hoechst 33342 was added to the media, and the cells were further cultured for 60 min. Hypoxia Green Reagent for Flow Cytometry is a membrane-permeant, fluorogenic probe that can help detect cells under a low oxygen status. As cellular oxygen concentration decreases, the probe releases rhodamine, which causes detectable emission in the green channel by flow cytometry. The cells were analyzed with FACS Aria and Flowjo (both BD Biosciences).

2.8 | Immunoblot analyses

Immunoblot was performed as described.¹⁵ Antibodies used were HIF-1 α , ab16066 (Abcam); heme oxygenase-1, D-8 (Santa Cruz Biotechnology); β -actin, AC-15 (Santa Cruz Biotechnology); FoxO3a, #12829 (Cell Signaling Technology); and anti-mouse IgG (H + L), AP conjugate secondary antibody (Promega).

2.9 | Quantitative RT-PCR

Random primer-based synthesized cDNA was analyzed by quantitative PCR using a real-time PCR system (Thermal Cycler Dice, Takara Bio Inc.) as described.¹⁶ Specific PCR was performed using gene-specific primers and SYBR Select Master Mix (Applied Biosystems). The levels of β -actin were quantified as an internal control. Quantitative PCR Primers (Target Gene, Sequence) used were HO-1-F, 5'-AGAAGAGCTGCACCGCAAGG-3'; HO-1-R, 5'-ATGGCTGGTGTAGGGGATG-3'; β -actin-F, 5'-TGG CAC CCA GCA CAA TGA A-3'; β -actin-R, 5'-CTA AGT CAT AGT CCG CCT AGA AGC A-3'.

2.10 | Preparation of stable cell transformants for HO-1 knockdown

The HO-1 target sequence was inserted into the CS-RfA-EVbSd vector (kindly provided by Dr H. Miyoshi, RIKEN BioResource Center)

for knockdown of the HO-1 gene. This plasmid or its control with a luciferase target sequence were transduced into HL cell lines as previously described,¹⁴ and Venus positive cells were sorted using FACS Aria (BD Biosciences). The knockdown effect in these transformants was confirmed using immunoblot. HO-1 target sequence for short hairpin (sh) RNA#1:5'-GGTTCTTGCACTTAGCTTT -3'; HO-1 target sequence for shRNA#2:5'-GGAGATTGAGTGCAGCAAA -3'.

2.11 | Microarray analyses of gene expression

We used the 4 \times 44K Whole Human Genome Oligo Microarray (Agilent Technologies); detailed methods were previously reported.¹⁷ The RNA from sorted SP or MP cells of HL cell lines was Cy3-labeled using a Low Input Quick Amp Labeling Kit (Agilent Technologies). Labeled cRNA samples were hybridized to 44K Whole Human Genome Oligonucleotide Microarrays (Agilent Technologies) at 65°C for 17 h, washed and scanned with a Scanner C (Agilent Technologies). Signal intensities were evaluated by Feature Extraction 10.7 software and analyzed using Gene Spring 13.0 software (Agilent Technologies).

For data analysis, we performed 75th percentile alignment (75% centering) of intensity distributions of all samples and removed very low signal values for appropriate normalization. Coordinates have been deposited to the Gene Expression Omnibus database with accession number GSE 142414.

GSEA (Gene Set Enrichment Analysis) was performed using the gene expression data for SP and MP cells of HL cell lines. Software used was GSEA v3.0. All gene set files for this analysis were obtained from the GSEA website (<http://software.broadinstitute.org/gsea/>).

2.12 | Statistical analysis

For statistical analysis of mean values, the experiments were performed at least three times independently. The results are presented as mean \pm SD in bar graphs, and the differences were assessed using a two-tailed *t* test. A *P* value $< .05$ was considered to be statistically significant. Spearman's correlation coefficient and *P* value were calculated after confirming the values were not followed for a normal distribution by SUITEXL software. A *P* value $< .05$ was considered to be statistically significant.

3 | RESULTS

3.1 | ROS levels are low in the SP compared to the MP in HL cell lines

To examine whether ROS commits the differentiation of HL cells, we first examined the concentration of intracellular ROS in the SP and the MP of HL cell lines using CM-H₂DCFDA (Thermo Fisher Scientific) by flow cytometry. A representative result of SP analysis

of the HL cell line and histograms for CM-H₂DCFDA are presented in Figure 1A,B. The mean fluorescence intensity (MFI) of CM-H₂DCFDA in the SP of HL cell lines was significantly lower than that of the MP cells (Figure 1C).

Since mitochondria are a major source of ROS, we further examined the activity of ROS production in mitochondria using MitoTracker Red CM-H₂XRos (Thermo Fisher Scientific) by flow cytometry. A representative result of SP analysis of fluorescent signals of the HL cell lines and histograms of MitoTracker Red CM-H₂XRos are presented in Figure 2A,B. The MFI in the SP of HL cell lines was significantly lower than that of the MP cells (Figure 2C).

To clarify whether the difference in ROS production in the SP and MP is caused by the activity or the number of mitochondria, we performed immunostaining of mitochondria in the SP and MP of HL cell lines. The results showed that there appeared to be no significant difference in the fluorescence intensity between the SP and MP cells (Figure 2D).

These results indicate that HL cells contain an immature fraction with low ROS levels and that an increase of ROS is associated with

a differentiated phenotype. The results also indicated that the increased production of ROS in the differentiated cells depends on the activity of mitochondria.

3.2 | Treatment of HL cell lines with hydrogen peroxide induces large mono- and multinucleated cells

To further address the roles of ROS in the differentiation of HL cells, we treated HL cell lines with hydrogen peroxide and observed its effect on cellular morphology. The treatment induced large, multinucleated cells (Figure 3A, top and middle). Results by other HL cell lines are presented in Figure S1. On the other hand, the treatment of an unrelated cell line, Namalwa, generated very small cells with condensed nuclei, indicating cell death (Figure 3A bottom).

To validate this observation, we performed analyses by flow cytometry in HL cell lines and found that treatment with hydrogen peroxide increased forward-scattered light (Figure 3B, left). We also analyzed with DNA histograms, and the results showed that

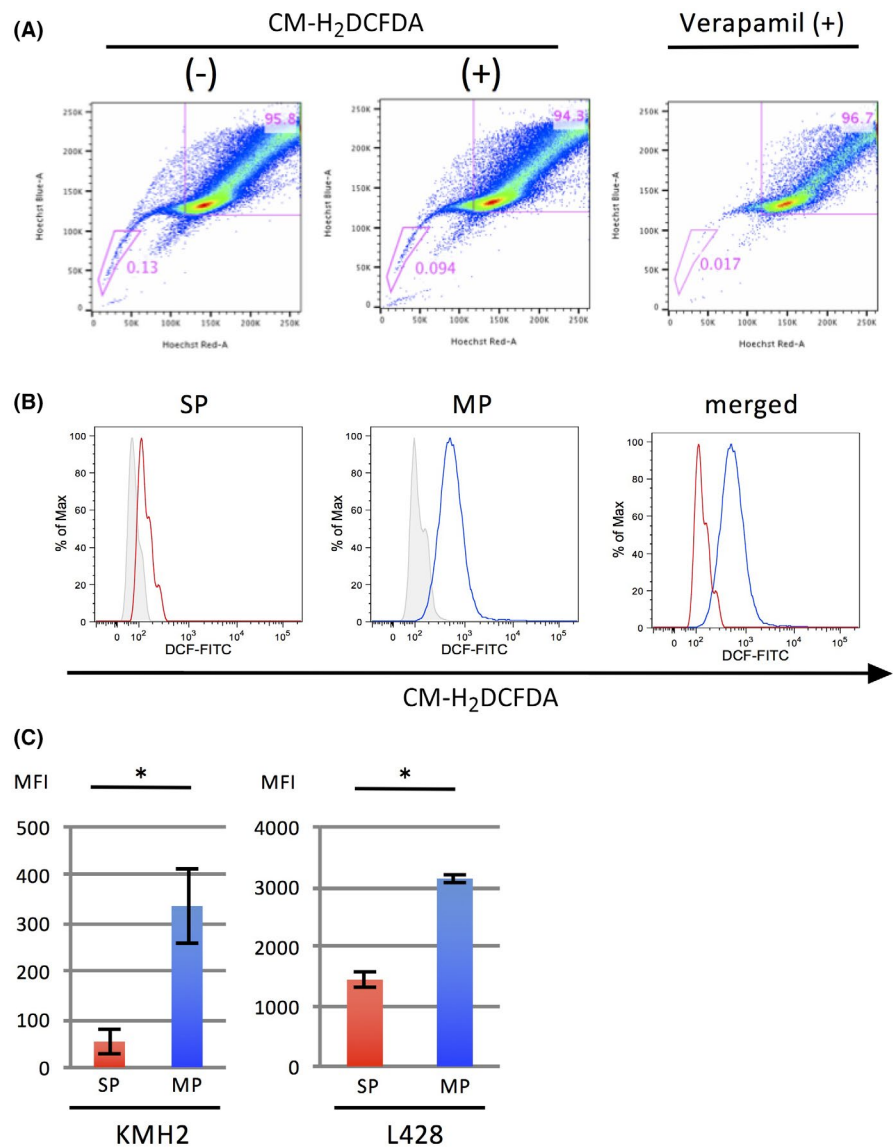


FIGURE 1 Intracellular ROS levels are lower in the SP compared to the MP in HL cell lines. A, Analysis of SP cells in an HL cell line, KMH2. The cells with or without treatment by CM-H₂DCFDA, an indicator of intracellular ROS production, are presented in the middle and on the left, respectively. The SP fraction is reduced by treatment with verapamil, a Ca²⁺ ion channel blocker (right). The percentage of SP cells is indicated in each graph. B, Histograms of CM-H₂DCFDA intensity in SP cells and MP cells are presented on the left and in the middle, respectively. The results from cells without treatment are indicated as gray shaded histograms. The histograms merged are shown on the right. C, Bar graphs of mean fluorescence intensity (MFI) of SP and MP cells of HL cell lines KMH2 and L428 treated with CM-H₂DCFDA. *, P < .05 [Correction added on 8 April 2021, after first online publication: In Figure 1, the text 'CH-H₂DCFDA' in 1A and 1B images has been corrected to 'CM-H₂DCFDA'.]

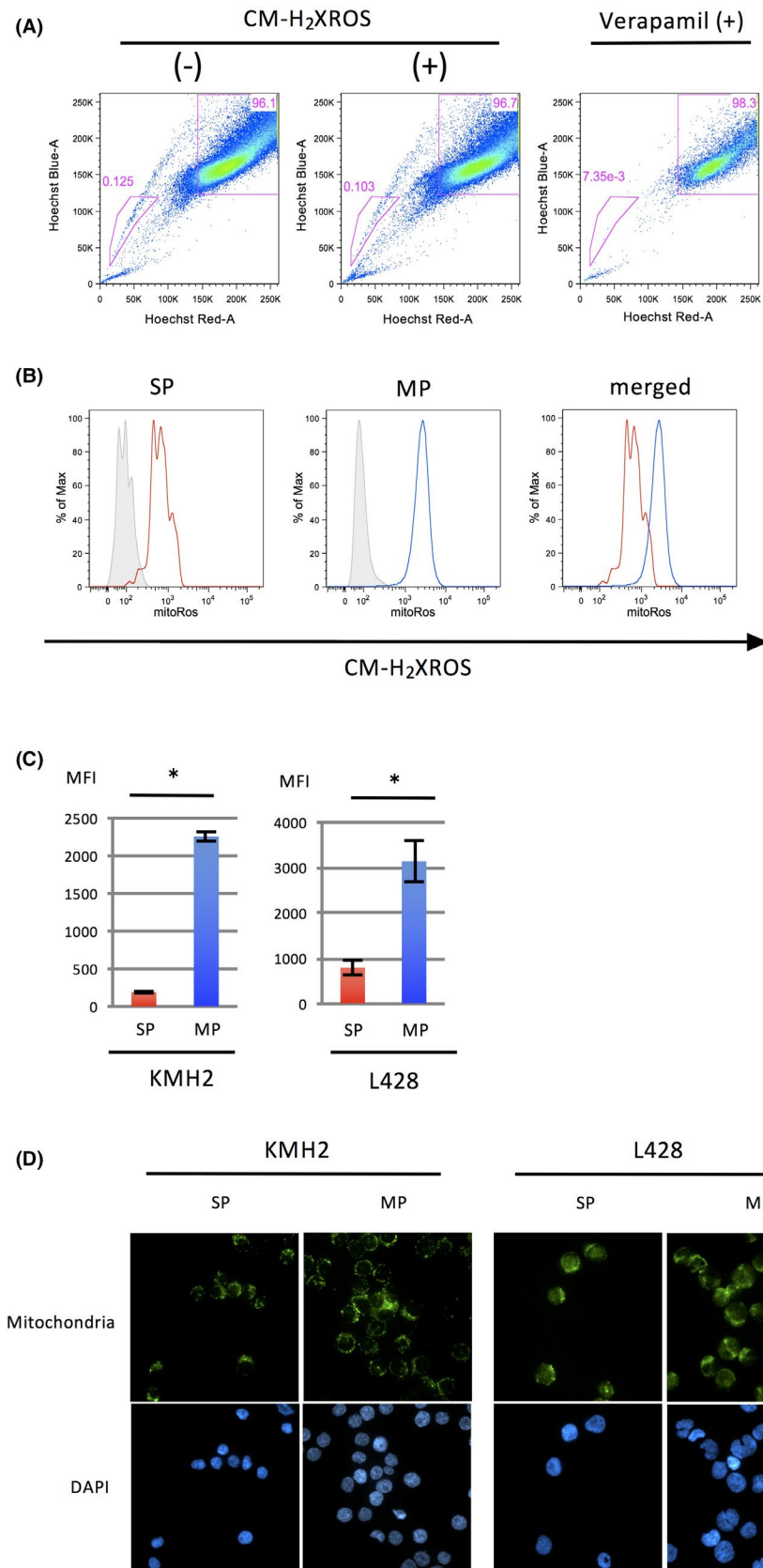
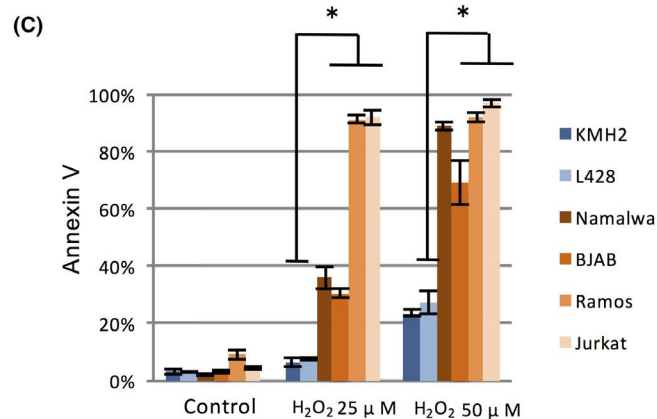
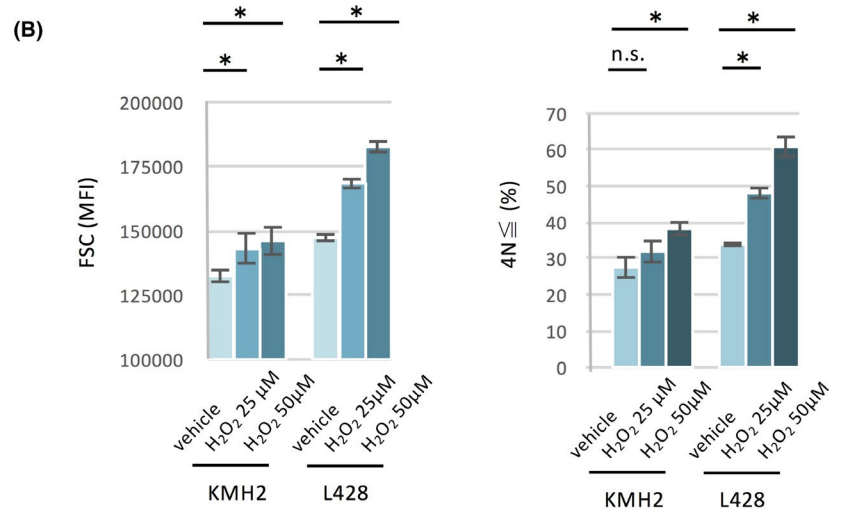
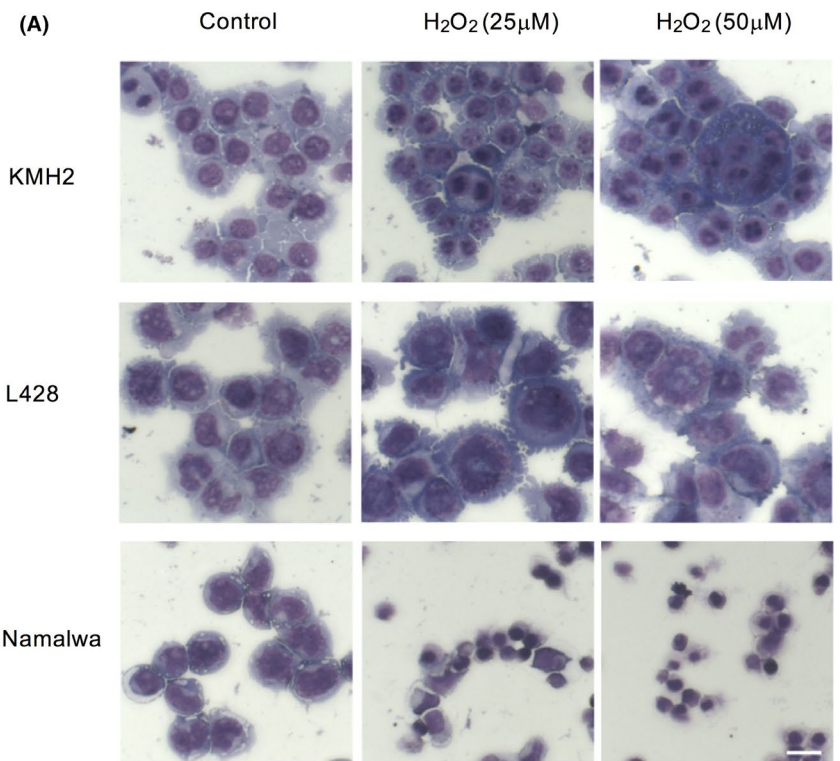


FIGURE 2 The MP of HL cell lines increased mitochondrial ROS compared to the SP. A, Analysis of SP cells in an HL cell line, L428. Cells with or without treatment by CM-H₂XROS, an indicator of mitochondrial ROS production, are presented in the middle and on the left, respectively. The SP fraction is reduced by treatment with verapamil, a Ca²⁺ ion channel blocker (right). The percentage of SP cells is indicated in each graph. B, Histograms of CM-H₂XROS intensity in SP and MP cells of L428 are presented on the left and the middle, respectively. Cells without treatment are indicated as gray shaded histograms. The histograms merged are shown at the right. C, Bar graphs of MFI of SP and MP cells of HL cell lines KMH2 and L428 treated with CM-H₂XROS. The experiments were performed three times independently. *, *P* < .05. D, Immunostaining of mitochondria in SP and MP cells of HL cell lines. SP and MP cells (5.0×10^4) of each cell line were sorted and cytopspun onto slides and stained with an anti-mitochondrial antibody (top). DAPI staining of each cell line is presented in the bottom panels. These cells were analyzed using fluorescence microscopy. Scale bar, 100 μ m

treatment of HL cell lines with hydrogen peroxide generated $\geq 4N$ cells (Figure 3B, right). We next examined whether hydrogen peroxide treatment of lymphoid cell lines unrelated to HL induced cell

death according to Annexin V. The percentage of Annexin V-positive cells after treatment with hydrogen peroxide was significantly higher in the unrelated cell lines compared to HL cell lines (Figure 3C).

FIGURE 3 Treatment of HL cell lines with hydrogen peroxide induces large mono- and multinuclear cells. A, Cellular morphology of HL cell lines (KMH2 and L428) and a non-HL cell line (Namalwa) treated with the indicated concentrations of hydrogen peroxide for 72 h. Scale bar, 20 μ m. B, Flow cytometric analyses of changes in cell size of HL cell lines treated with hydrogen peroxide for 48 h. The vertical axis indicates MFI of forward-scattered light (left). Ploidy analysis of HL cell lines treated with hydrogen peroxide for 48 h; the vertical axis indicates the $\geq 4N$ cells (cells with DNA content of tetraploid or more) rate from PI-negative total live cells (right). * $P < .05$. C, HL cell lines retain resistance to cytotoxic effects by hydrogen peroxide. HL cell lines (KMH2 and L428) and non-HL cell lines (Namalwa, BJAB, Ramos, and Jurkat) were treated with hydrogen peroxide for 48 h, and the expression of Annexin V was detected by flow cytometry. * $P < .05$



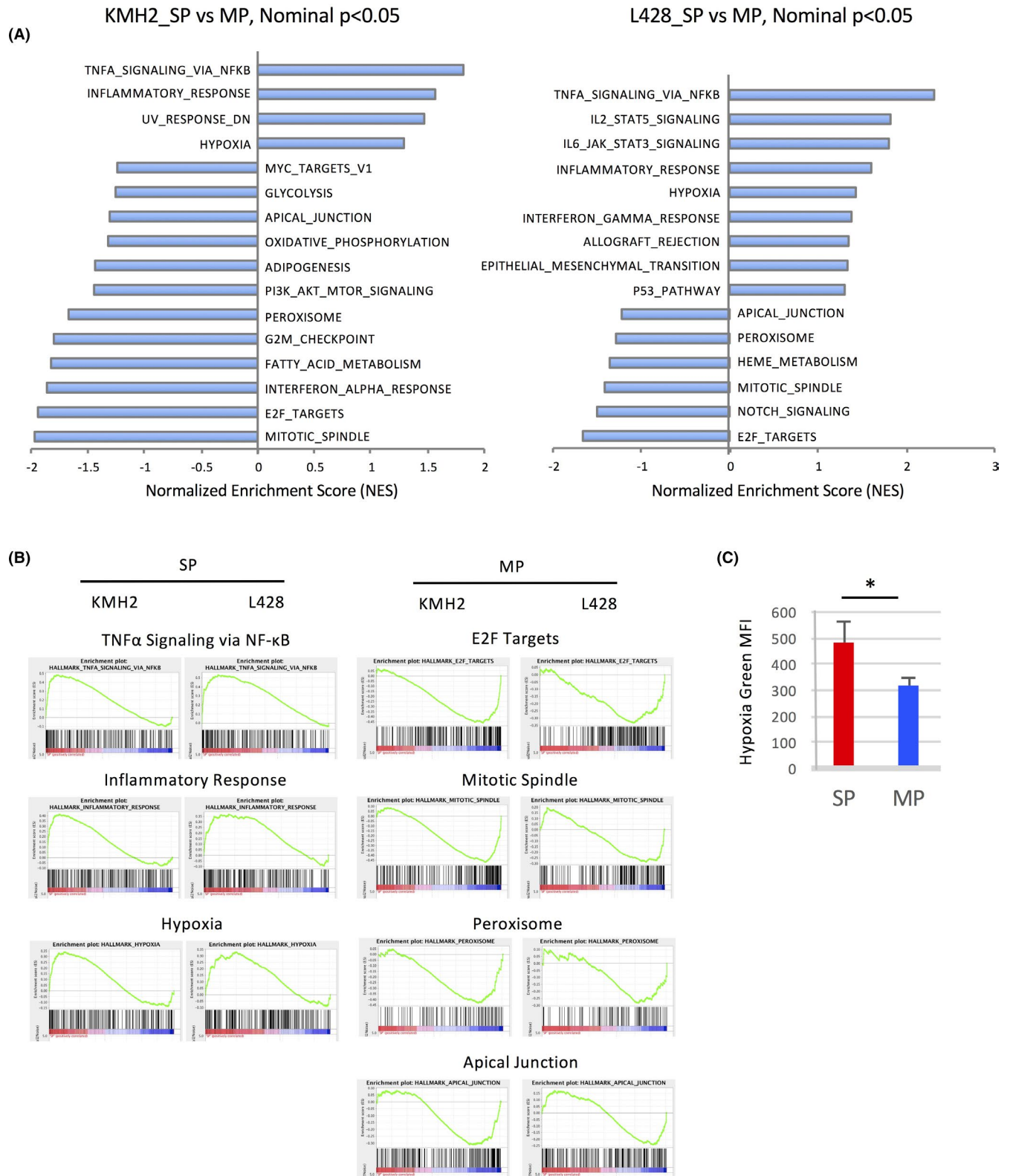


FIGURE 4 Microarray analyses of gene expression in SP and MP cells of HL cell lines. A, Analysis of hallmarks of gene expression comparing SP cells with MP cells. Gene set enrichment analysis (GSEA) was calculated using hallmark gene sets in MSigDB. The hallmarks within nominal $P < .05$ are presented as bar graphs of the normalized enrichment score (NES) order. NES-positive score indicates hallmarks of SP cells, while NES-negative score indicates those of MP cells (left KMH2, right L428). B, The common hallmark gene sets calculated by GSEA within nominal $P < .05$ in SP cells and MP cells of HL cell lines. These gene sets of SP cells (left) and MP cells (right) are presented as graphical panels outputted by GSEA. C, Measurement of hypoxic status in SP and MP cells of KMH2 using Hypoxia Green Reagent for flow cytometry, a hypoxic cell indicator. * $P < .05$

Combined with the higher intracellular ROS in the differentiated cells, the results above suggest that ROS directly induces the differentiation of HL cells. The results also show that this effect appears to be unique to HL cells among lymphoid cells.

3.3 | Microarray analyses of gene expression in the SP and MP of HL cell lines

To elucidate why the intracellular concentration of ROS is low in the SP compared to the MP, we first examined the profiles of gene expression by microarray analysis. Gene Set Enrichment Analysis (GSEA) using hallmark gene sets in the Molecular Signatures Database (MSigDB) showed significant differences ($P < .05$) between SP and MP cells in HL cell lines. These gene sets are displayed in a GSEA normalized enrichment score (NES) order for each cell line (Figure 4A).¹⁸ Common gene sets detected with a significant difference ($P < .05$) are presented as graphical figures in Figure 4B. This analysis shows that the SP cells in the HL cell lines are characterized by upregulation of genes related to “TNF- α Signaling via NF- κ B”, “Inflammatory Response”, and “Hypoxia” compared to the MP cells.

GSEA based on the microarray suggested that the SP cells in HL cell lines had upregulation of hypoxia-related genes. This gene set in MSigDB is composed of 200 genes, is refined in four dataset references, and is upregulated in response to low oxygen levels (http://software.broadinstitute.org/gsea/msigdb/cards/HALLMARK_HYPOXIA.html). Based on this, we wanted to measure the hypoxic status using a hypoxia-detecting probe. First, we confirmed that this probe could detect various oxygen concentrations in our experimental conditions using a multigas incubator (MCO-18M, SANYO Electric Biomedical Co., Ltd) (Figure S2A,B). Then we measured the oxygen concentration of SP and MP cells in the HL cell line and found that the SP cells were hypoxic compared to the MP cells (Figure 4C). A representative result of SP analysis and fluorescent signals is presented in Figure S3A,B.

Since “TNF- α Signaling via NF- κ B” is upregulated in the SP compared to the MP and previous reports indicated the cross-talk of NF- κ B and ROS,¹⁹ we examined the effect of NF- κ B inhibition on the ROS production of the SP and the MP cells of HL cell lines using an NF- κ B inhibitor Jietacin A.¹³ However, there was no significant change in the ROS level of the SP and MP cells after the treatment with Jietacin A. The results of the KMH2 cell line are presented in Figure S4A,B.

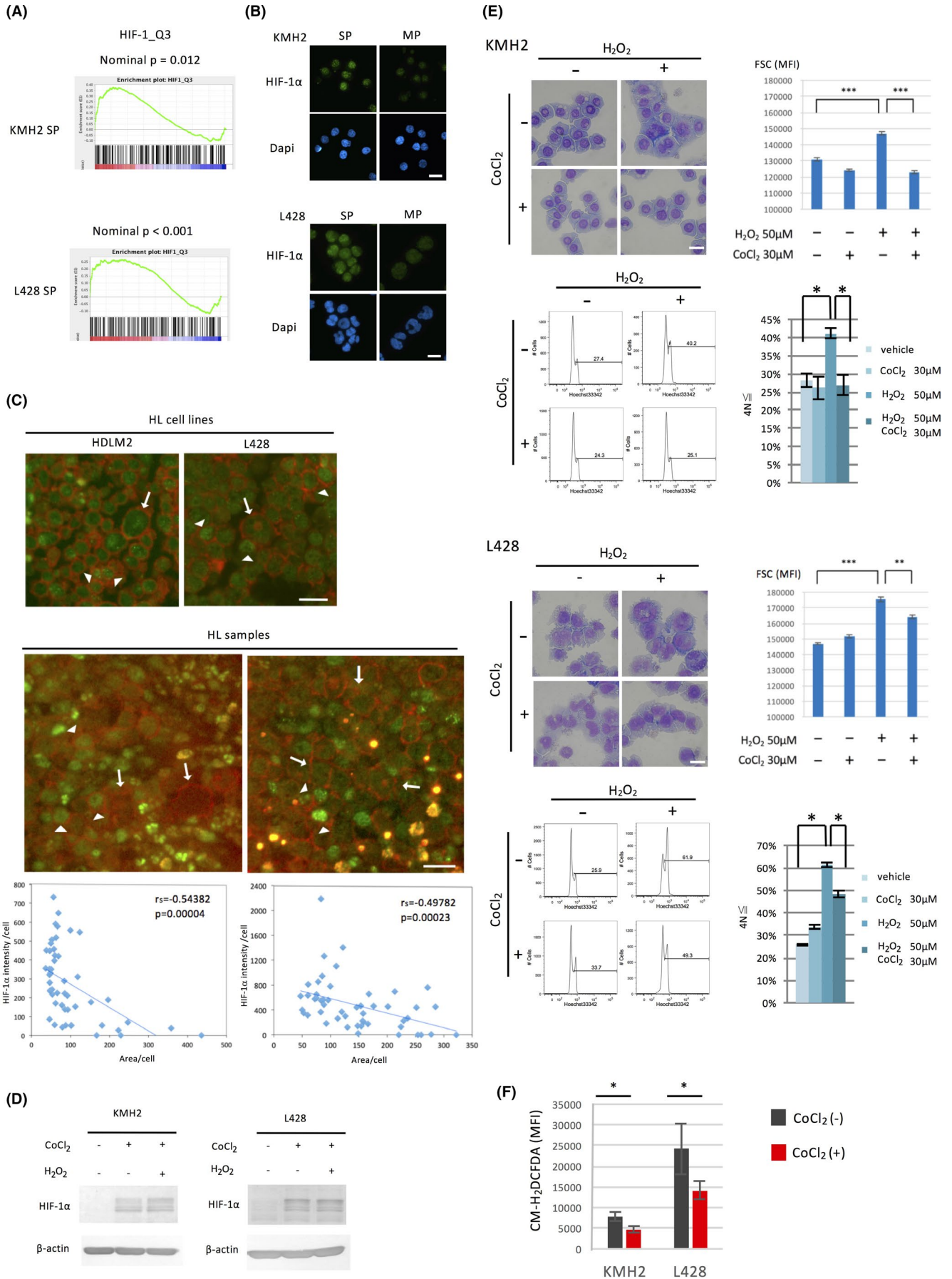
3.4 | HIF-1 α , preferentially expressed in SP cells, prevents ROS-mediated generation of large and hyperploid cells in HL cell lines

Previous reports indicated that the expression of HIF-1 α , which is induced under hypoxic conditions, is preferentially induced in stem cells. HIF-1 α has been reported to inhibit ROS production by inhibiting the citrate acid pathway in mitochondria and inducing antioxidant defenses during hypoxia.²⁰⁻²²

Furthermore, GSEA based on the expression profile showed that SP cells in HL cell lines are significantly enriched with upregulated genes with HIF-1 binding motifs on their promoter regions whose dataset in MSigDB is composed of 230 genes (Figure 5A; http://software.broadinstitute.org/gsea/msigdb/cards/HIF1_Q3.html).

We therefore examined the change of expression of HIF-1 α during HL cell differentiation. Immunostaining showed that HIF-1 α is more strongly expressed in SP cells compared to MP cells (Figure 5B). We previously showed Hodgkin (H) cells in the affected lymph nodes consist of various sizes and indicated that immature H cells reveal morphologically smaller cells.² H and RS cells selectively express high levels of CD30 in the affected lymph nodes of HL.²³ Therefore, we performed double immunofluorescence staining of CD30 and HIF-1 α in tissue samples of HL patients. The HL cell lines served as reference (Figure 5C, top) and representative results are shown in Figure 5C (bottom). Similar to the HL cell lines, among cells

FIGURE 5 HIF-1 α , preferentially expressed in the SP, prevents ROS-mediated differentiation of HL cell lines. A, GSEA comparing SP cells with MP cells using the gene set HIF1_Q3, which includes 230 genes with HIF-1 binding motifs on their promoter regions. B, Analysis of the expression of HIF-1 α in SP and MP cells of HL cell lines. The cells were sorted by flow cytometry, cytospun onto glass slides, and stained with an anti-HIF-1 α antibody. The nuclei were stained with DAPI. Scale bar, 50 μ m. C, Analysis of the expression of HIF-1 α in H and RS cells of HL samples by immunostaining of HIF-1 α and CD30. The staining of the HL cell lines used as reference is shown (top). The representative results from five samples examined are presented (bottom). Among cells stained by anti-CD30 antibody Ber-H2, arrows and arrowheads show large cells with weak HIF-1 α staining and smaller cells with strong HIF-1 α staining, respectively. Scale bar, 20 μ m. Integrated fluorescent intensity for HIF-1 α per each cell was calculated (50 cells) by measurement of the area of each cell stained with anti-CD30 antibody as strong as giant RS cells and by the mean fluorescent intensity by ImageJ software. When the mean fluorescent intensity of the area is equal or less than that of the background, the intensity was set to 0. Scatter plots for the area and the intensity with linear regression lines are presented below each immunofluorescence staining image. *rs*, Spearman's correlation coefficient. D, Analysis of the expression of HIF-1 α by CoCl₂ and hydrogen peroxide (H₂O₂). HL cell lines (1×10^5 /mL) were cultured with or without the HIF-1 α stabilizer, CoCl₂ (30 μ mol/L), and hydrogen peroxide (50 μ mol/L) for 24 h, then harvested and used for immunoblot analysis. E, Inhibition of ROS-mediated differentiation of HL cell lines by the induction of HIF-1 α . HL cell lines were cultured with or without CoCl₂ (30 μ mol/L) and hydrogen peroxide (50 μ mol/L) for 48 h. The morphological changes were examined using the May-Giemsa method and flow cytometry (top left and right of each HL cell line). Scale bar, 50 μ m. Ploidy of the cells was analyzed using flow cytometry, and representative DNA histograms are shown (bottom left of each HL cell line). The percentage of the $\geq 4N$ cells was calculated as described in Figure 3B (bottom right of each HL cell line). * $P < .05$, ** $P < .01$, *** $P < .001$. F, Effect of CoCl₂ on intracellular ROS production in HL cell lines. HL cell lines were cultured with or without CoCl₂ (30 μ mol/L) for 24 h. Intracellular ROS production was measured using CM-H₂DCFDA by flow cytometry. MFI is shown as bar graphs. * $P < .05$



stained with anti-CD30 antibody as strong as giant RS cells, HIF-1 α is generally stained strongly in smaller H cells. The intensity for HIF-1 α was negatively correlated to the area of these CD30-positive cells and the results were presented below each immunofluorescence staining image. Collectively these results support the notion that the expression of HIF-1 α protein is relatively strong in the immature fraction of HL cells and its expression decreases in the differentiated large HL cells.

We next examined whether HIF-1 α inhibits the differentiation of HL cells. We examined the effect of the HIF-1 α stabilizer CoCl₂ on HIF-1 α in HL cell lines. Treatment of HL cell lines with CoCl₂ induced HIF-1 α and hydrogen peroxide did not affect this induction (Figure 5D). Stabilization of HIF-1 α by CoCl₂ inhibited hydrogen peroxide-mediated generation of large cells (Figure 5E, top left and right of each HL cell line examined) and hyperploid cells (Figure 5E, bottom left of each HL cell line examined). According to the percentage of the $\geq 4N$ cells, HIF-1 α clearly prevented hydrogen peroxide-mediated generation of polyploid HL cells (Figure 5E, bottom right of each HL cell line examined).

To test whether the effects shown in Figure 5E were associated with a reduction of ROS, we measured the concentration of intracellular ROS by flow cytometry using CM-H₂DCFDA. The results showed a reduction of the MFI after CoCl₂ treatment, suggesting the effects were caused by a reduction of ROS (Figure 5F).

Collectively, these results suggest that HIF-1 α is preferentially expressed in SP cells, diminishing the intracellular concentration of ROS and preventing ROS-mediated differentiation of HL cells.

3.5 | HO-1 is induced by HIF-1 α , and its inhibition promotes the generation of hyperploid cells and intracellular ROS in HL cell lines

We further addressed how intracellular ROS levels are regulated during the differentiation of HL cells. Since the induction of HIF-1 α appears to

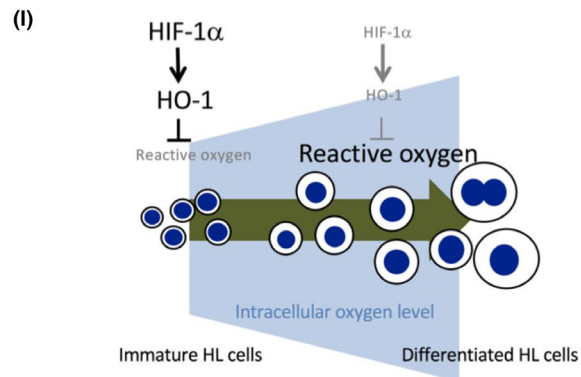
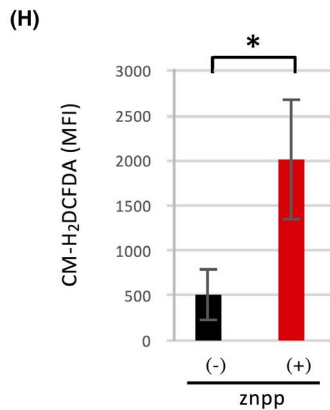
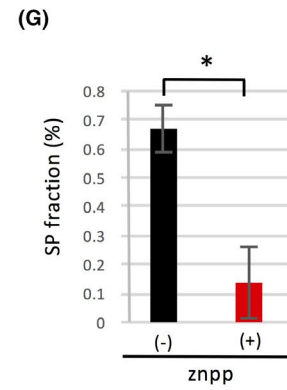
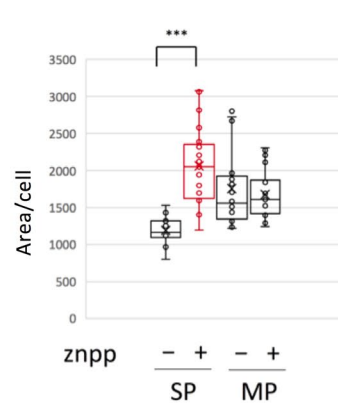
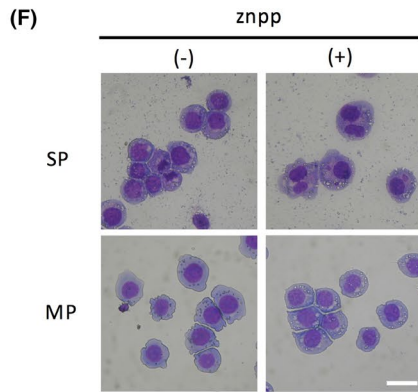
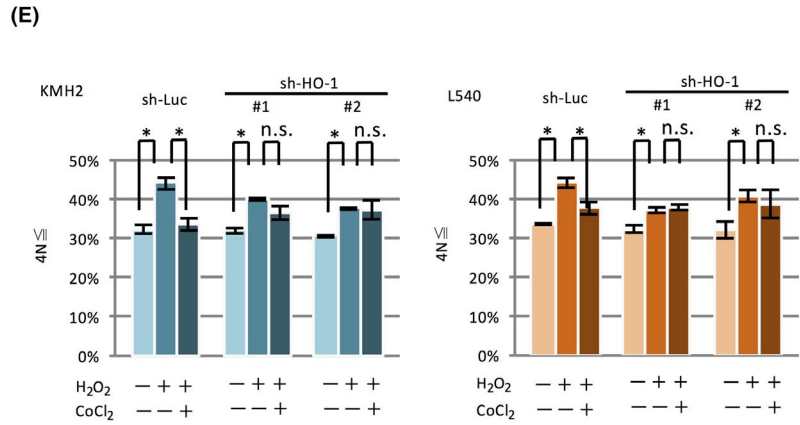
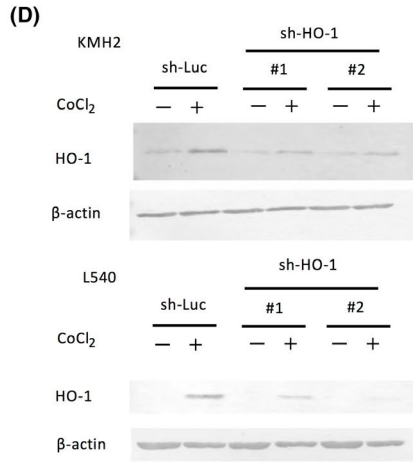
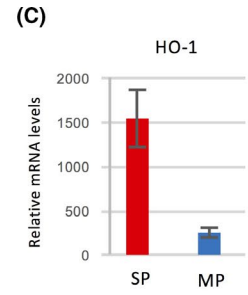
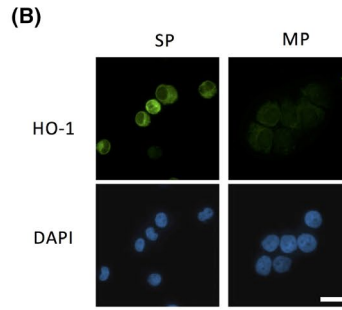
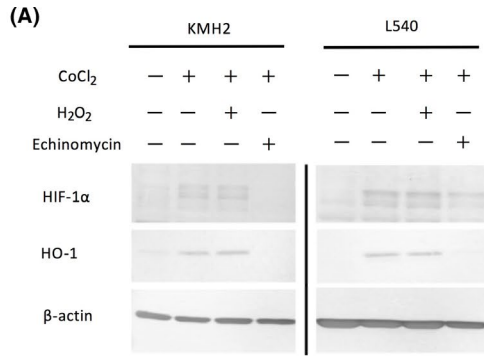
prevent ROS-mediated differentiation of HL cell lines, we next focused on antioxidants that are induced by HIF-1 α . Among them, we examined the roles of HO-1,²² which is a strong scavenger of ROS triggered by HIF-1 α that commits cells to tumor progression.²⁴⁻²⁷

We examined whether HO-1 induction is dependent on HIF-1 α in HL cell lines. CoCl₂, a HIF-1 α stabilizer, induced HO-1, whereas echinomycin, an HIF-1 α inhibitor, decreased HO-1 expression (Figure 6A). We failed to detect HO-1 protein in the HL cell line L428. L428 expressed a truncated form of HO-1 mRNA, which might have prevented detection by immunoblot (data not shown). To clarify the roles of HO-1 in the differentiation of HL cells, we examined the expression of HO-1 in SP and MP cells. The expression of HO-1 in the SP was stronger than that in the MP (Figure 6B,C).

We next examined whether the differentiation of HL cells is dependent on HO-1. For this purpose, we prepared stable shRNA transformants of HO-1 and confirmed their knockdown (Figure 6D). We then examined the effect of HO-1 knockdown on differentiation as measured by the generation of the $\geq 4N$ cells after treatment with hydrogen peroxide. HO-1 knockdown abolished the effect of CoCl₂ (Figure 6E). The SP fraction was not decreased in the shRNA transformant of HO-1, suggesting the existence of a compensatory mechanism to maintain the SP (Figure 5S).

Finally, we treated the SP cells of the HL cell line with znpp, an inhibitor of HO-1, and examined its effect on differentiation as measured by morphological changes. The results showed that znpp treatment promoted the emergence of large mono- or binucleated cells (Figure 6F, left) and increased the area of each cell (Figure 6F, right). The treatment with znpp also reduced the SP fraction (Figure 6G). Since HO-1 is a scavenger of ROS, we measured the increase of ROS in SP cells after treatment with znpp. The results showed a significant increase in the concentration of intracellular ROS in the SP (Figure 6H).

FIGURE 6 HO-1 levels are high in the SP of HL cell lines, and its inhibition induces hyperploidy and multinuclear cells. A, Induction of HO-1 by CoCl₂. HL cell lines were cultured with or without CoCl₂ (30 μ mol/L) for 24 h, then harvested and used for immunoblot analysis. Under treatment with CoCl₂, the effect of the HIF-1 α inhibitor echinomycin (KMH2 100 nmol/L, L540 2 nmol/L) or hydrogen peroxide (50 μ mol/L) on HO-1 expression was also examined. B, Analysis of HO-1 expression between SP and MP cells of KMH2. SP and MP cells of KMH2 were sorted by flow cytometry, cytospun onto glass slides, and stained with anti-HO-1 antibody. The nuclei were stained with DAPI, and the cells were analyzed by fluorescence microscopy. Scale bar, 50 μ m. C, Relative HO-1 expression levels between SP and MP cells of KMH2. SP and MP cells were sorted by flow cytometry, and the expression of mRNA was analyzed by qRT-PCR. HO-1 expression levels relative to β -actin measured by duplicated experiments are shown as bar graphs. D, Analysis of HO-1 gene knockdown using short hairpin RNA (shRNA). HL cell lines were transduced with lentivirus expressing shRNA against the HO-1 gene (sh-HO-1 #1 and #2) or experimental control (sh-Luc) as described in the Materials and Methods section. These cells were cultured with CoCl₂ (30 μ mol/L) for 24 h, then harvested and used for immunoblot analysis. E, Ploidy analysis in HL cell lines expressing shRNA against HO-1. HL cell lines expressing shRNA against HO-1 or sh-Luc control were cultured with CoCl₂ (30 μ mol/L) for 24 h, then harvested and used for measurement of ploidy. The ploidy of the cells was analyzed using flow cytometry, and the percentage of the $\geq 4N$ cells was calculated as described and shown as bar graphs. * $P < .05$. n.s., not significant. F, Morphological changes by znpp in SP cells. SP and MP cells of KMH2 were sorted by flow cytometry, and each cell type was then treated with znpp (5 μ mol/L) for 24 h. The cells were harvested, cytospun onto glass slides, and stained by the May-Giemsa method (left). Scale bar, 50 μ m. Each area of the cells was measured by ImageJ and the results are presented by box plots (right). *** $P < .001$. G, Effect of znpp on the percentage of SP fraction. The percentage of SP cells in KMH2 with or without znpp (5 μ mol/L) was analyzed using flow cytometry. * $P < .05$. H, Effect of znpp on ROS of SP cells. Intracellular ROS levels of SP cells of KMH2 with or without znpp (5 μ mol/L) were analyzed using flow cytometry. The vertical axis indicates MFI of CM-H₂DCFDA, an intracellular ROS indicator. * $P < .05$. I, Schematic representation of the regulation of HL cell differentiation by reactive oxygen through HIF-1 α



Taken collectively, these results indicate that HO-1, an antioxidant induced by HIF-1 α , is more strongly expressed in the immature fraction of HL cells and prevents ROS-mediated differentiation.

3.6 | The stabilization of HIF-1 α does not enhance the expression of FoxO3a and does not reduce the production of mitochondrial ROS in HL cell lines

Previous reports indicated the existence of small tumorigenic cells with low ROS and high FoxO3a in HL cells.¹ Another report suggested that FoxO3a induction is dependent on HIF-1 α and reduces intracellular ROS by inhibiting the suppression of mitochondrial activity.^{28,29} We therefore examined the relationship between HIF-1 α and FoxO3a in HL cell lines. The expression level of FoxO3a mRNA appears to be relatively high in the SP, but did not show statistical significance (Figure S6A). We could not find a clear difference in the expression of FoxO3a between the small and large cells of HL cell lines (Figure S6B). Furthermore, the stabilization of HIF-1 α neither induced pyruvate dehydrogenase kinase (PDK)-1 activation, which inhibits transition of glycolysis to aerobic tricarboxylic acid (TCA) cycle, nor reduced mitochondrial ROS (data not shown).

4 | DISCUSSION

The results in this study suggest that the intracellular concentration of ROS dynamically affects transition of the SP to the MP and is involved in the differentiation of HL cells. Although treatment of HL cell lines with hydrogen peroxide promoted differentiation, the same treatment of other T- and B-cell lines tested did not. This is in accordance with the notion that ROS causes pleiotropic effects including proliferation, differentiation, and apoptosis.⁶ On this point, ROS-mediated differentiation appears to be a unique property of HL cells.

We demonstrated that SP cells of HL cell lines were enriched in hypoxia-related genes by microarray-based comprehensive expression analysis. We also showed directly that the SP cells were hypoxic compared to the MP cells. These results are supported by a previous report showing that hypoxia enhances tumor stemness by increasing the tumorigenic side population fraction.³⁰ A hypoxic tumor microenvironment is known to be important in the regulation of cancer stem cell characteristics.³¹ A recent report has indicated that cancer stem-like cells derived from a hypoxic tumor microenvironment maintain stem cell features even in aerobic conditions.³² Our results show that the SP cells of HL cell lines are hypoxic and have elevated HIF-1 α expression, although they are cultured in aerobic conditions. Therefore, our results indicate that the immature fraction of cancer cells retains cellular mechanisms to maintain hypoxia independent of the extracellular environment, although elucidating the responsible molecular mechanisms requires further study.

We showed that the expression of HIF-1 α is elevated in SP cells. We also indicated the expression of HIF-1 α is relatively strong in the

immature fraction of HL cells and its expression decreases during the differentiation. We suggested that smaller H cells retain higher HIF-1 α expression compared to giant RS cells in biopsied samples of lymph nodes. However, some smaller H cells appear to reveal low HIF-1 α expression. This might suggest that these cells have entered the differentiation phase, although further analyses are required. Identification of markers specific for the SP cells of HL and experiments using them will enable us to strengthen the findings in this study. This will help us to clarify the localization of the stem cell-like fraction of HL in the body.

Stabilization of HIF-1 α inhibited hydrogen peroxide-mediated differentiation of HL cell lines. We demonstrated that this inhibition is mediated by HO-1, a strong scavenger of ROS²⁴⁻²⁷ situated downstream of HIF-1 α .²² One HL cell line, L428, expressed a truncated form of HO-1 mRNA, and we could not detect the HO-1 protein. Since L428 revealed high HIF-1 α expression in SP cells and its stabilization also inhibited their differentiation, other ROS scavenger proteins might contribute to the regulation of ROS.

Mitochondria are a major source of ROS.^{33,34} We found that the expression of HIF-1 α is higher in the immature fraction of HL cells. A previous report indicated that HIF-1 α inhibits mitochondrial activity and ROS production through activation of PDK-1.³⁵ However, we could not detect activation of PDK-1 under stabilization of HIF-1 α . The stabilization of HIF-1 α failed to suppress the generation of mitochondrial ROS, suggesting that ROS production in mitochondria is independent of the expression of HIF-1 α in HL cells. Although constitutively strong activation of NF- κ B is a feature of HL cells,² we indicated that NF- κ B appears not to be involved in the regulation of ROS and the differentiation in these cells.

Our results indicate that immature HL cells antagonize differentiation by a reduction of ROS not thorough direct inhibition of mitochondrial activity, but through HO-1 induction by HIF-1 α . ROS impairs the function of mitochondria and becomes a cause of further generation of ROS.^{36,37} Thus, it is possible that breakdown of ROS regulation by HO-1 via HIF-1 α might increase ROS from mitochondria and promote the differentiation of HL cells.

Previous reports have indicated the existence of small tumorigenic cells with low ROS and high FoxO3a in HL cells.³ FoxO3a is reported to inhibit ROS by repressing a set of nuclear-encoded mitochondrial genes.²⁸ However, we did not find significant differences in FoxO3a between the SP and MP of HL cell lines, suggesting that FoxO3a involvement in the regulation of ROS in HL cells is unlikely.

In summary, the results of this study stress the unique roles of ROS in the differentiation of HL cells. Schematic representation of this study is presented in Figure 6I. Immature HL cells antagonize differentiation by reducing ROS through the induction of HO-1 via HIF-1 α . Its breakdown may then increase intracellular ROS and promote the differentiation of HL cells.

ACKNOWLEDGMENTS

Flow cytometric analysis was supported technically by the FACS Core Laboratory, Center for Stem Cell Biology and Regenerative Medicine, Institute of Medical Science, University of Tokyo. Multigas

incubator was kindly provided by Satoshi Yamazaki and Kiyosumi Ochi at the Division of Stem Cell Biology, Institute of Medical Science, University of Tokyo. An NF- κ B inhibitor, Jietacin A, was kindly provided by Toshiaki Sunazuka at the Ōmura Satoshi Memorial Institute and Graduate School of Infection Control Sciences, Kitasato University. This work was supported in part by a MEXT/JSPS KAKENHI grant to RH (17K08728 and 20K07379), MW (19K07442) and MN (19K16580), and a Japan Agency for Medical Research and Development (AMED) grant to KU (19fk0108039h0003 and 20fk0108126h0001).

CONFLICTS OF INTEREST

All authors declare no potential conflicts of interest.

ORCID

Ryouichi Horie  <https://orcid.org/0000-0002-2431-2290>

REFERENCES

- Ikeda J, Mamat S, Tian T, et al. Tumorigenic potential of mononucleated small cells of Hodgkin lymphoma cell lines. *Am J Pathol*. 2010;177(6):3081-3088.
- Nakashima M, Ishii Y, Watanabe M, et al. The side population, as a precursor of Hodgkin and Reed-Sternberg cells and a target for nuclear factor-kappaB inhibitors in Hodgkin's lymphoma. *Cancer Sci*. 2010;101(11):2490-2496.
- Ikeda J, Mamat S, Tian T, et al. Reactive oxygen species and aldehyde dehydrogenase activity in Hodgkin lymphoma cells. *Lab Invest*. 2012;92(4):606-614.
- Valko M, Leibfritz D, Moncol J, Cronin MT, Mazur M, Telser J. Free radicals and antioxidants in normal physiological functions and human disease. *Int J Biochem Cell Biol*. 2007;39(1):44-84.
- Murphy MP. How mitochondria produce reactive oxygen species. *Biochem J*. 2009;417(1):1-13.
- Zhou D, Shao L, Spitz DR. Reactive oxygen species in normal and tumor stem cells. *Adv Cancer Res*. 2014;122:1-67.
- Ito K, Hirao A, Arai F, et al. Reactive oxygen species act through p38 MAPK to limit the lifespan of hematopoietic stem cells. *Nat Med*. 2006;12(4):446-451.
- Trachootham D, Alexandre J, Huang P. Targeting cancer cells by ROS-mediated mechanisms: a radical therapeutic approach? *Nat Rev Drug Discov*. 2009;8(7):579-591.
- Gopas J, Stern E, Zurgil U, et al. Reed-Sternberg cells in Hodgkin's lymphoma present features of cellular senescence. *Cell Death Dis*. 2016;7(11):e2457.
- Singh M, Sharma H, Singh N. Hydrogen peroxide induces apoptosis in HeLa cells through mitochondrial pathway. *Mitochondrion*. 2007;7(6):367-373.
- Yang G, Nguyen X, Ou J, Rekulapelli P, Stevenson DK, Dennery PA. Unique effects of zinc protoporphyrin on HO-1 induction and apoptosis. *Blood*. 2001;97(5):1306-1313.
- Kong D, Park EJ, Stephen AG, et al. Echinomycin, a small-molecule inhibitor of hypoxia-inducible factor-1 DNA-binding activity. *Cancer Res*. 2005;65(19):9047-9055.
- Watanabe M, Sugawara A, Noguchi Y, et al. Jietacins, azoxy natural products, as novel NF-kappaB inhibitors: discovery, synthesis, biological activity, and mode of action. *Eur J Med Chem*. 2019;178:636-647.
- Nakashima M, Yamochi T, Watanabe M, et al. CD30 characterizes polylobated lymphocytes and disease progression in HTLV-1 infected individuals. *Clin Cancer Res*. 2018;24(21):5445-5457.
- Nakashima M, Watanabe M, Uchimar K, Horie R. Trogocytosis of ligand-receptor complex and its intracellular transport in CD30 signalling. *Biol Cell*. 2018;110(5):109-124.
- Takahashi R, Yamagishi M, Nakano K, et al. Epigenetic deregulation of Ellis Van Creveld confers robust Hedgehog signaling in adult T-cell leukemia. *Cancer Sci*. 2014;105(9):1160-1169.
- Kobayashi S, Nakano K, Watanabe E, et al. CADM1 expression and stepwise downregulation of CD7 are closely associated with clonal expansion of HTLV-I-infected cells in adult T-cell leukemia/lymphoma. *Clin Cancer Res*. 2014;20(11):2851-2861.
- Liberzon A, Birger C, Thorvaldsdottir H, Ghandi M, Mesirov JP, Tamayo P. The Molecular Signatures Database (MSigDB) hallmark gene set collection. *Cell Syst*. 2015;1(6):417-425.
- Morgan MJ, Liu ZG. Crosstalk of reactive oxygen species and NF-kappaB signaling. *Cell Res*. 2011;21(1):103-115.
- Kim JW, Tchernyshyov I, Semenza GL, Dang CV. HIF-1-mediated expression of pyruvate dehydrogenase kinase: a metabolic switch required for cellular adaptation to hypoxia. *Cell Metab*. 2006;3(3):177-185.
- Kirito K, Hu Y, Komatsu N. HIF-1 prevents the overproduction of mitochondrial ROS after cytokine stimulation through induction of PDK-1. *Cell Cycle*. 2009;8(17):2844-2849.
- Lee PJ, Jiang BH, Chin BY, et al. Hypoxia-inducible factor-1 mediates transcriptional activation of the heme oxygenase-1 gene in response to hypoxia. *J Biol Chem*. 1997;272(9):5375-5381.
- Schwartz R, Gerdes J, Durkop H, Falini B, Pileri S, Stein H. BER-H2: a new anti-Ki-1 (CD30) monoclonal antibody directed at a formol-resistant epitope. *Blood*. 1989;74(5):1678-1689.
- Ryter SW, Alam J, Choi AM. Heme oxygenase-1/carbon monoxide: from basic science to therapeutic applications. *Physiol Rev*. 2006;86(2):583-650.
- Doi K, Akaike T, Fujii S, et al. Induction of haem oxygenase-1 nitric oxide and ischaemia in experimental solid tumours and implications for tumour growth. *Br J Cancer*. 1999;80(12):1945-1954.
- Nuhn P, Kunzli BM, Hennig R, et al. Heme oxygenase-1 and its metabolites affect pancreatic tumor growth in vivo. *Mol Cancer*. 2009;8:37.
- Was H, Cichon T, Smolarczyk R, et al. Overexpression of heme oxygenase-1 in murine melanoma: increased proliferation and viability of tumor cells, decreased survival of mice. *Am J Pathol*. 2006;169(6):2181-2198.
- Jensen KS, Binderup T, Jensen KT, et al. FoxO3A promotes metabolic adaptation to hypoxia by antagonizing Myc function. *EMBO J*. 2011;30(22):4554-4570.
- Bakker WJ, Harris IS, Mak TW. FOXO3a is activated in response to hypoxic stress and inhibits HIF1-induced apoptosis via regulation of CITED2. *Mol Cell*. 2007;28(6):941-953.
- Das B, Tsuchida R, Malkin D, Koren G, Baruchel S, Yeger H. Hypoxia enhances tumor stemness by increasing the invasive and tumorigenic side population fraction. *Stem Cells*. 2008;26(7):1818-1830.
- Lin Q, Yun Z. Impact of the hypoxic tumor microenvironment on the regulation of cancer stem cell characteristics. *Cancer Biol Ther*. 2010;9(12):949-956.
- Kim H, Lin Q, Glazer PM, Yun Z. The hypoxic tumor microenvironment in vivo selects the cancer stem cell fate of breast cancer cells. *Breast Cancer Res*. 2018;20(1):16.
- Jezeq P, Hlavata L. Mitochondria in homeostasis of reactive oxygen species in cell, tissues, and organism. *Int J Biochem Cell Biol*. 2005;37(12):2478-2503.
- Cheng Z, Ristow M. Mitochondria and metabolic homeostasis. *Antioxid Redox Signal*. 2013;19(3):240-242.
- Ishimoto T, Nagano O, Yae T, et al. CD44 variant regulates redox status in cancer cells by stabilizing the xCT subunit of system xc(-) and thereby promotes tumor growth. *Cancer Cell*. 2011;19(3):387-400.

36. Cline SD. Mitochondrial DNA damage and its consequences for mitochondrial gene expression. *Biochim Biophys Acta*. 2012;1819(9-10):979-991.
37. Pinto M, Moraes CT. Mechanisms linking mtDNA damage and aging. *Free Radic Biol Med*. 2015;85:250-258.

SUPPORTING INFORMATION

Additional supporting information may be found online in the Supporting Information section.

How to cite this article: Nakashima M, Watanabe M, Nakano K, Uchimaru K, Horie R. Differentiation of Hodgkin lymphoma cells by reactive oxygen species and regulation by heme oxygenase-1 through HIF-1 α . *Cancer Sci*. 2021;112:2542-2555. <https://doi.org/10.1111/cas.14890>